NASA TECHNICAL NOTE

NASA TN D-3252

NASA TN D-3252

FRACTURE MECHANICS OF THROUGH-CRACKED CYLINDRICAL PRESSURE VESSELS

by Robert B. Anderson and Timothy L. Sullivan

Lewis Research Center
Cleveland, Ohio

NATIONAL AERONAUTICS AND SPACE ADMINISTRATION • WASHINGTON, D. C. • FEBRUARY 1966

NASA TN D-3252

FRACTURE MECHANICS OF THROUGH-CRACKED CYLINDRICAL PRESSURE VESSELS

By Robert B. Anderson and Timothy L. Sullivan

Lewis Research Center
Cleveland, Ohio

NATIONAL AERONAUTICS AND SPACE ADMINISTRATION

For sale by the Clearinghouse for Federal Scientific and Technical Information
Springfield, Virginia 22151 – Price $2.00

FRACTURE MECHANICS OF THROUGH-CRACKED CYLINDRICAL PRESSURE VESSELS

by Robert B. Anderson and Timothy L. Sullivan

Lewis Research Center

SUMMARY

The application of some fracture mechanics concepts to the prediction of the strength of pressure vessels in which cracks have penetrated entirely through the vessel wall is examined. The strength of cylindrical pressure vessels (with longitudinal through-cracks) is related to the geometry of the cylinder, the crack length, the material yield strength, and fracture toughness. An expression for the crack tip stress intensity factor is derived by considering the influence on the stress near the crack tip of membrane stressing in the cylinder and of bending caused by bulging of the partially constrained material on either side of the crack. The form of the derived expression is verified and empirical constants evaluated from burst data at -320° and -423° F of aluminum alloy (2014-T6 Al) and extra-low-interstitial (ELI) titanium alloy (5Al-2.5Sn-Ti) tanks.

The analysis, based on the Irwin fracture theory, provides a suitable means for the correlation of the strength of flat-sheet specimens with that of cracked pressurized cylinders. The correlation suggests that the fracture strength of through-cracked cylinders of any radius, crack length, and thickness can be determined from material toughness, yield strength, and a bulge coefficient. Neglect of the effect of pressure bulging in the fracture analysis of pressurized cylinders can cause a significant overestimate of the fracture strength.

INTRODUCTION

The presence of cracks in the wall of a pressure vessel, such as a cryogenic liquid rocket propellant tank, can severely reduce the strength of the structure and can cause sudden failure at nominal tensile stresses less than the material yield strength. In such cases, cracks form at inherent flaws in the structure, extend under loading to a critical size, and then propagate rapidly through the material. To ensure the integrity of a structure when a flaw is present requires that the designer understand and adequately consider the mechanics of fracture, particularly the relation between fracture load and the flaw and structural geometry.

G. R. Irwin has developed a useful fracture analysis that relates the stress distribution near the tip of a crack to the Griffith energy criteria for unstable crack growth (ref. 1). This analysis relates the fracture load to the size of the crack, the geometry of the structure, and a single material fracture toughness parameter. The Irwin analysis has been applied to various structural and crack configurations including tensioned flat plates having through cracks (ref. 2) or surface cracks (ref. 3), edge-cracked beams in bending and tension (ref. 4), and surface-cracked pressurized cylinders (ref. 5). Although a fracture analysis of a pressurized cylinder in which a crack has penetrated entirely through the vessel wall is not available, there is evidence that the strength of through-cracked pressurized cylinders is less than that of a flat sheet having the same crack size. This behavior was discussed by Peters and Kuhn in reference 6, which reports results of burst tests of through-cracked aluminum cylinders.

The present work examines this apparent reduction in cylinder burst strength through the application of fracture mechanics concepts. The strength reduction is considered to be due to an increase in the crack tip stress intensity caused by pressure bulging near the crack. The stress intensity factor associated with bulging is derived by a dimensional analysis, and the Griffith-Irwin fracture criterion is employed to relate circumferential stress at fracture to crack length, cylinder radius, material fracture toughness, yield strength, and an empirical bulge coefficient. Data from burst tests of cylinders of 2014-T6 Al and ELI 5Al-2.5Sn-Ti at -320° and -423° F verify the form of the expression for fracture strength.

SYMBOLS

$2a$	crack length, in.
$2a_c$	critical crack length, in.
$2a_g$	crack length indicated by continuity gage, in.
$2a_o$	initial crack length, in.
C	dimensionless bulge coefficient
C_i	set of experimental bulge coefficient values
E	Young's modulus, psi
$\mathcal{E}$	fractional error in fracture toughness value due to material inconsistencies
K	stress intensity factor, psi $\sqrt{\text{in.}}$
K_b	stress intensity factor associated with pressure bulging, psi $\sqrt{\text{in.}}$
K_c	critical stress intensity factor, fracture toughness, psi $\sqrt{\text{in.}}$

K_{cn}	nominal fracture toughness (based on initial crack length), psi $\sqrt{\text{in.}}$
K_h	stress intensity factor associated with membrane hoop stressing in pressurized cylinder, psi $\sqrt{\text{in.}}$
k	dimensionless coefficient, eq. (2)
p	pressure, psi
R	radius of cylinder, in.
r	coordinate distance from crack tip in crack plane, in.
r_{fg}	distance from crack tip to location of failure in continuity gage, in.
r_p	length of plastic zone at crack tip, in.
S_u	stress concentration factor for cracked flat sheet
$S_{u, cyl}$	stress concentration factor for cracked cylinder
t	sheet thickness, in.
W	sheet width, in.
w_i	least-squares method weighting factors
$\alpha, \beta, \gamma, \delta, \lambda$	dimensionless exponents, eq. (2)
ϵ_{fg}	failure strain of continuity gage, in./in.
ϵ_y	strain ahead of crack and normal to crack plane, in./in.
ϵ_{yY}	strain ahead of crack and normal to crack plane at elastic-plastic interface, in./in.
σ	uniform gross stress acting normal to plane of crack, psi
σ_c	critical uniform gross stress acting normal to plane of crack, psi
σ_h	membrane hoop stress in cylinder, psi
σ_{hc}	critical membrane hoop stress, psi
σ_l	membrane longitudinal stress in cylinder, psi
σ_Y	uniaxial yield strength, psi
σ_{YB}	yield strength in 2:1 biaxial stress field, psi
σ_y	stress ahead of crack and normal to crack plane, psi
σ_{yb}	surface tensile bending stress normal to crack plane ahead of crack, psi
σ_{yY}	stress ahead of crack and normal to crack plane at elastic-plastic interface, psi

ANALYSIS

Fracture Criterion

The stress distribution near a crack in a structure can be described by a linear elastic stress analysis, provided that plastic deformation is confined to a small region near the tip of the crack. G. R. Irwin (ref. 7) and M. L. Williams (ref. 8) have shown that the stress near the end of a crack in a linear-elastic material is inversely proportional to the square root of the distance from the crack tip. For example, the stress ahead of the crack and normal to the crack plane, σ_y, varies with distance r from crack tip by $\sigma_y = \frac{K}{\sqrt{2\pi r}}$ for small r. The constant of proportionality in this relation is the stress intensity factor K, which expresses the magnitude of the stress field near the crack tip. The stress intensity factor is a function of the applied load, the crack size and shape, and the geometry of the structure.

Irwin (ref. 1) has related the stress intensity factor to the rate of release of elastic strain energy with crack extension, which according to the Griffith theory of fracture reaches a critical value at fracture. Consequently, a fracture criterion is formulated in terms of the stress intensity factor: Fracture occurs when K attains a critical value K_c, usually termed the fracture toughness of the material. Values of K_c can be obtained from laboratory tests of suitable precracked specimens by methods discussed in detail in references 2 and 4. By use of the Irwin fracture criterion the strength of a structure containing a crack can be determined from the fracture toughness of the material and the dimensions of the crack and of the structure.

Application of this criterion to through-cracked cylindrical pressure vessels requires an expression for the stress intensity factor which includes the special geometrical and loading conditions pertinent to this kind of structure. If such an expression were known, the strength of a cracked cylinder could be determined from its dimensions, the length of the crack, and the toughness of the material.

Stress Intensity Factor for a Through-Cracked Cylindrical Pressure Vessel

The stress intensity near the end of a through crack in a pressurized cylinder is considered to be influenced by two distinct loading mechanisms - membrane stressing in the cylinder wall and bending caused by bulging of the partially constrained material on either side of the crack. The following analysis examines the stress intensity associated with each of these loading effects for the case of a longitudinal crack of length 2a located in a cylinder as shown in figure 1. The segment of the cylinder wall which contains

the crack is represented in figure 2(a) as a sheet subjected to uniform lateral pressure p and normal stresses σ_h and σ_l, corresponding to hoop and longitudinal stresses, respectively. The stress intensity factor K_h due to hoop stress σ_h is assumed to be that of a centrally cracked wide sheet subjected to a remote uniform tensile stress. According to reference 3, K_h can be expressed by

$$K_h = \sigma_h \sqrt{\pi a} \tag{1}$$

The contribution of the longitudinal stress σ_l to the stress intensity is considered to be negligible as discussed in reference 2.

The influence of lateral pressure on the stress intensity can be inferred by considering the effects of pressure on the material on either side of the crack. Pressure against the partially constrained portion of the tank wall near the crack would cause deflection and rotation of the crack edge as shown in figure 2(b). Since the rotation is zero at the crack tip, a restraining bending moment occurs ahead of the crack thereby introducing a bending stress normal to the crack plane. The surface tensile bending stress ahead of the crack, designated σ_{yb}, is assumed to be a function of distance from the crack tip r, pressure p, sheet thickness t, Young's modulus E, and crack length 2a. In the absence of an explicit relation between σ_{yb} and this set of variables, it is assumed that σ_{yb} close to the crack tip can be expressed in the functional form

$$\sigma_{yb}(p, E, a, t, r) = k p^{\alpha} E^{\beta} a^{\gamma} t^{\delta} r^{\lambda} \tag{2}$$

where k is a dimensionless coefficient and α, β, γ, δ, and λ are dimensionless exponents. Correct dimensionality of equation (2) requires that $\beta = 1 - \alpha$ and $\gamma = -(\delta + \lambda)$ or

$$\sigma_{yb} = kE\left(\frac{p}{E}\right)^{\alpha}\left(\frac{a}{t}\right)^{-\delta}\left(\frac{r}{a}\right)^{\lambda} \tag{3}$$

The exponents α and λ can be evaluated from the following known aspects of the mechanics of the problem. Since the material is linearly elastic, the bending stress is proportional to the pressure, whereby in equation (3), $\alpha = 1$. In all linear-elastic crack problems the stress near the crack tip varies inversely with the square root of the distance from the crack tip (refs. 7 and 8). Thus λ must equal -1/2. For later convenience, let $-\delta$ equal a dimensionless number μ. Equation (3) can now be written as

$$\sigma_{yb} = kp\left(\frac{a}{r}\right)^{1/2}\left(\frac{a}{t}\right)^{\mu} \tag{4}$$

The stress σ_y near the tip of a crack is related to the stress intensity factor K in reference 2 by

$$K = \sigma_y \sqrt{2\pi r} \tag{5}$$

Consequently, the bending stress σ_{yb} close to the crack tip can be related to a stress intensity factor associated with pressure bulging K_b by

$$K_b = \sigma_{yb} \sqrt{2\pi r} \tag{6}$$

Then from equations (4) and (6) this bulge stress intensity factor is related to pressure, crack length, and sheet thickness by

$$K_b = Cp \sqrt{\pi a} \left(\frac{a}{t}\right)^{\mu} \tag{7}$$

where C is a dimensionless coefficient equal to $k\sqrt{2}$.

For cases in which both membrane stressing and pressure bulging occur near a crack, the total stress intensity is the sum of the stress intensities for each of the loading conditions, since stress intensity factors can be superimposed for a given crack length. In the special case of a pressurized cylinder having a crack oriented parallel to its axis, the total stress intensity factor K is the sum of the stress intensity factor due to hoop membrane stressing K_h and that due to bulging K_b; that is,

$$K = K_h + K_b \tag{8}$$

From equations (1), (7), and (8),

$$K = \sigma_h \sqrt{\pi a} + Cp \sqrt{\pi a} \left(\frac{a}{t}\right)^{\mu} \tag{9}$$

Equation (9) is a stress intensity factor for a cracked plate element under uniform tensile stress σ_h and lateral pressure p. When this element is considered to be a segment of the cylinder wall, $p = \sigma_h t/R$ for a cylinder of radius R, and equation (9) becomes

$$K = \sigma_h \sqrt{\pi a} \left[1 + C \frac{t}{R} \left(\frac{a}{t}\right)^{\mu}\right] \tag{10}$$

At fracture, K equals K_c, 2a equals the critical crack length $2a_c$, and σ_h equals the critical hoop stress σ_{hc}, which, from equation (10), is

$$\sigma_{hc} = \frac{K_c}{\sqrt{\pi a_c} \left[1 + C \frac{t}{R} \left(\frac{a_c}{t}\right)^{\mu}\right]} \tag{11}$$

It should be noted that as R becomes very large, equation (11) reduces to the expression for the critical stress on a wide flat sheet, which according to reference 2 is

$$\sigma_c = \frac{K_c}{\sqrt{\pi a_c}} \tag{12}$$

In this expression the crack length is usually altered to account for the effect of plastic deformation at the tip of the crack by replacing a_c with $a_c + \frac{K_c^2}{2\pi\sigma_Y^2}$ (ref. 9) where σ_Y is the uniaxial yield strength. If a similar plasticity correction is used in the corresponding square root term in equation (11), the critical hoop stress becomes

$$\sigma_{hc} = \frac{K_c}{\sqrt{\pi a_c + \frac{1}{2} \frac{K_c^2}{\sigma_{YB}^2}} \left[1 + C \frac{t}{R} \left(\frac{a_c}{t}\right)^{\mu}\right]} \tag{13}$$

where σ_{YB} is the yield strength in a 2:1 biaxial stress field. This expression relates the critical hoop stress in a cracked pressurized cylinder to crack length, wall thickness, cylinder radius, yield strength, and fracture toughness. In equation (13) the crack length in the bulge term $C \frac{t}{R} \left(\frac{a_c}{t}\right)^{\mu}$ was not modified for plastic deformation because the resulting expression would indicate a finite bulge effect at zero crack length.

The form of equation (13) can be verified and the values of μ and C obtained from experimental data from burst tests of precracked cylinders. When equation (13) is

rewritten as

$$\psi = C\left(\frac{a_c}{t}\right)^{\mu-1} \tag{14}$$

where

$$\psi = \frac{R}{a_c}\left(\frac{\frac{K_c}{\sigma_{hc}}}{\sqrt{\pi a_c + \frac{1}{2}\frac{K_c^2}{\sigma_{YB}^2}}} - 1\right)$$

the parameters C and μ can be separated by taking the logarithm of each side of equation (14):

$$\ln \psi = (\mu - 1)\ln \frac{a_c}{t} + \ln C \tag{15}$$

This expression predicts a linear relation between ψ and a_c/t on a log-log plot. Burst tests of pressurized cylinders are required to test this relation and to evaluate the parameters μ and C.

APPARATUS AND PROCEDURE

The validity of the form of equation (13) was investigated using data from burst tests of cylinders of four different materials having various thicknesses, radii, and crack lengths, at room temperature, -320°, and -423° F. Fracture data for 2014-T6 Al and ELI 5Al-2.5Sn-Ti were obtained at the Lewis Research Center from tests of 6-inch-diameter cylinders such as that shown in figure 3 having longitudinal notches or cracks varying in length from 0.1 to 2.0 inches. The 2014-Al cylinders were cut from extruded tubing, heat treated to the T6 condition, and machined to a wall thickness of 0.060 inch (ref. 10). The roots of the notches in the aluminum cylinders were machined to a radius of about 0.0002 inch. The aluminum nominal fracture toughness values were obtained from tensile specimens that were cut from flattened tube stock that had been heat treated with the cylinders. These specimens, as that shown in figure 4, were 3 inches wide,

0.060 inch thick, and had 1-inch central notches machined to approximately 0.0002 inch radius at the root.

The titanium cylinders were formed from 0.020-inch sheet material with a single longitudinal butt weld. Each cylinder was stress-relieved by heating to 1100° F for 2 hours. Cracks were started by extending half-wall-thickness electrical discharge notches through the wall by low-stress pressure cycling. Fatiguing was continued until the cracks reached the desired test length. The 3-inch-wide titanium toughness specimens were made from the same sheet stock as that used for the cylinders and were subjected to the same heat treatment and crack preparation.

Room temperature data for two aluminum alloys (2024-T3 and 7075-T6 Al) were obtained from results of notched cylinder burst tests published in reference 6. These data represent cylinder radii of 3.6 and 14.4 inches, wall thicknesses ranging from 0.006 to 0.025 inch, and crack lengths varying from 0.24 to 7.70 inches.

The direction of testing for both the 2014-T6 Al and ELI 5Al-2.5Sn-Ti toughness specimens corresponded to the hoop direction in the cylinders. During loading of the toughness specimens and the cylinders, slow crack extension was monitored by electrical resistance foil element continuity gages (ref. 11) placed at the crack tip. These gages consisted of 20 elements connected in parallel and were mounted normal to the crack as shown in figure 5. As the crack grew individual elements broke causing an abrupt measurable resistance change. In the toughness tests, the initial crack length $2a_o$, the critical crack length $2a_c$, and the critical applied stress were measured. Fracture toughness values were calculated from these data by the expression given in reference 2

$$K_c = \sigma_c \sqrt{W \tan\left[\frac{\pi}{W}\left(a_c + \frac{1}{2\pi}\frac{K_c^2}{\sigma_Y^2}\right)\right]} \tag{16}$$

where W is the sheet width. Because there were cases in which the critical crack length was not known, an alternate correlation was based on the initial crack length, and a nominal fracture toughness K_{cn} was computed by

$$K_{cn} = \sigma_c \sqrt{W \tan\left[\frac{\pi}{W}\left(a_o + \frac{1}{2\pi}\frac{K_{cn}^2}{\sigma_Y^2}\right)\right]} \tag{17}$$

Although exact values of K_{cn} for the 2024-T3 and 7075-T6 Al sheet used in the tests of reference 6 are not available, typical toughness values of 90 000 psi$\sqrt{\text{inch}}$ for the 2024-T3

and 53 000 psi $\sqrt{\text{inch}}$ for the 7075-T6 Al were used in the computations. These values were estimated from flat sheet strength data included in reference 12.

In the burst tests of 2014-T6 Al and ELI 5Al-2.5Sn-Ti cylinders measurements were made of the initial crack, the critical pressure, and the critical crack length as indicated by the continuity gages. The gage-indicated crack length was subsequently corrected to obtain a more accurate critical crack length measurement, as discussed in appendix A. Table I summarizes pertinent cylinder burst test data.

Values of biaxial yield strength σ_{YB} of the aluminum were calculated from the Von Mises yield criterion to be 1.15 σ_Y for a 2:1 stress field. Because some titanium alloys exhibit significant increase in biaxial yield strength relative to uniaxial yield strength, values of σ_{YB} of ELI 5Al-2.5Sn-Ti were obtained from pressure tests of uncracked cylinders.

Data from the cracked cylinder burst tests were used to verify the expression for fracture strength developed in the ANALYSIS section as given by equation (15). The form of this expression was tested and the empirical parameters μ and C evaluated by plotting experimental values of ψ against a/t on a log-log plot. The values of ψ were computed for each cracked cylinder burst test using R, σ_{hc}, and a_o or a_c for each test and K_{cn} or K_c from the flat sheet toughness tests.

RESULTS AND DISCUSSION

The expression for the burst strength of through-cracked pressurized cylinders given by equation (15) in the ANALYSIS section indicates a linear relation between the terms ψ and a/t on a log-log graph. The plots of experimental values of ψ against a/t in figure 6 verify the predicted linear relation. In addition, for each case shown in figure 6 it appears that ψ is insensitive to the ratio a/t. The data indicate that ψ is constant over three decades of the ratio a/t, that is, the slope of the line, $\mu - 1$, is zero. This behavior suggests that in equation (15) the empirical constant C equals ψ and can be computed from the data using equation (14)

$$C = \frac{R}{a_c}\left(\frac{\frac{K_c}{\sigma_{hc}}}{\sqrt{\pi a_c + \frac{1}{2}\frac{K_c^2}{\sigma_{YB}^2}}} - 1\right) \tag{18}$$

for correlation based on the critical crack length or by

$$C = \frac{R}{a_o}\left(\frac{\frac{K_{cn}}{\sigma_{hc}}}{\sqrt{\pi a_o + \frac{1}{2}\frac{K_{cn}^2}{\sigma_{YB}^2}}} - 1\right) \tag{19}$$

for correlation based on the initial crack length.

Weighted averages of the experimental values of the empirical bulge coefficient C were computed by the method discussed in appendix B and are shown by solid lines in figures 6 and 7. The value of C obtained from the data of reference 6 is the unweighted mean of the data. The number thus obtained is approximately the same as the coefficient of a/R reported in reference 6 in which the ratio of the stress concentration factor for a cracked cylinder to that for a cracked flat sheet was found empirically to be

$$\frac{S_{u,\,cyl}}{S_u} = 1 + 9.2\,\frac{a}{R}$$

In that report the coefficient 9.2 was calculated from a comparison of the strength of cracked flat sheets to the strength of pressurized cylinders having the same crack lengths.

From examination of figure 7 it appears that the bulge coefficient C tends to decrease with decreasing temperature. At the present time it is not clearly understood why C is temperature or material dependent. Further investigation is required to explain this dependency.

The scatter of the data in figures 6 and 7 can be shown to be caused by an error in the half crack length a of ±0.02 inch and a total error in fracture toughness of ±4 percent for the aluminum and ±6 percent for the titanium. The fractional error in C due to both of these errors is derived in appendix C. The dashed curves on either side of the weighted mean values of C in figure 7 represent the computed deviation in C due to the estimated errors in crack length and fracture toughness. Because these curves bound almost all of the data, the scatter is accounted for by the errors cited previously.

Figures 8 to 10 are curves of fracture strength of pressurized cylinders computed as a function of crack length by the following expressions obtained from equations (18) or (19):

$$\sigma_{hc} = \frac{K_c}{\sqrt{\pi a_c + \frac{1}{2}\frac{K_c^2}{\sigma_{YB}^2}\left(1 + C\frac{a_c}{R}\right)}} \tag{20}$$

or

$$\sigma_{hc} = \frac{K_{cn}}{\sqrt{\pi a_o + \frac{1}{2}\frac{K_{cn}^2}{\sigma_{YB}^2}\left(1 + C\frac{a_o}{R}\right)}} \tag{21}$$

The curves in figures 8 to 10 were computed from equations (20) or (21) using toughness values obtained from flat sheet tests and the weighted mean C values from figure 7. The dashed curves in these figures are the upper and lower values of fracture strength prediction due to the experimental error in C discussed previously. The excellent correlation in these figures suggests that for a given material and temperature the fracture strength of cylinders of any radius, crack length, or wall thickness can be determined from as few cylinder burst tests as are necessary to obtain a meaningful value of the bulge coefficient C.

Neglect of the effects of pressure bulging will lead to an overestimate of the strength, as can be seen in figures 8 to 10 by comparing the fracture strength curves that include the bulge term to those that do not. It is apparent that there can be a large reduction in the strength of cracked cylinders due to pressure bulging, particularly for larger values of $C\frac{a}{R}$.

(Copy figures on pages 29, 30, 31 and 32)

CONCLUSIONS

The fracture mechanics analysis of the effects of pressure bulging near the crack on the stress intensity factor, as described in this report, provides an explanation for the lower strength of cracked cylinders relative to flat sheets as well as a method for correlating the strength of cracked pressurized cylinders with that of flat sheets.

Application of a fracture analysis of through-cracked pressurized cylinders that does not include the effects of pressure bulging could result in an overestimate of the fracture strength.

The close agreement between the form of the derived expression for fracture strength and the experimental data suggests that the fracture strength of cylinders of any radius, crack length, and wall thickness can be determined from material toughness, yield strength, and the bulge coefficient obtained from tests of a few cylinders.

Lewis Research Center,
National Aeronautics and Space Administration,
Cleveland, Ohio, October 1, 1965.

APPENDIX A

CALCULATION OF CORRECTED CRACK LENGTH FROM CONTINUITY GAGE DATA

In the cylinder burst tests and fracture toughness tests, the crack lengths indicated by the foil continuity gages were found to be longer than the actual crack length because the continuity gage elements failed slightly ahead of the actual crack front. Consequently, a more accurate measurement of crack length required a calibration of the continuity gages. The following theoretical calibration relates the gage-indicated crack length to a corrected crack length in terms of applied stress, material yield strength, yield strain, gage failure strain, and specimen width. It is presumed that the gage elements failed ahead of the crack because the ductility of the gage mounting cement was less than that of the specimen material. How this behavior might affect the gage readings is shown in figure 11, a sketch of strain ahead of a crack. When a gage element breaks at a strain ϵ_{fg}, it indicates a crack longer than the actual surface crack by an amount $2r_{fg}$. If the gage indicates a crack of length $2a_g$, the actual crack length is

$$2a = 2a_g - 2r_{fg} \tag{A1}$$

The distance r_{fg} is related to the length of the plastic region r_p, the strain at the elastic-plastic interface ϵ_{yY}, and the failure strain of the continuity gage ϵ_{fg} by a simplified approximation of the expression for strain ahead of a crack given in equations 2-43 to 2-45 of reference 13. Then

$$\frac{\epsilon_y}{\epsilon_{yY}} = 1 + \left(\frac{\pi}{2}\right)^4 \left(\sqrt{\frac{r_p}{r}} - 1\right) \qquad r < r_p \tag{A2}$$

Equation (A2) can be solved for r_{fg} by noting that $r = r_{fg}$ at $\epsilon_y = \epsilon_{fg}$. Thus,

$$r_{fg} = \left[1 + \left(\frac{2}{\pi}\right)^4 \left(\frac{\epsilon_{fg}}{\epsilon_{yY}} - 1\right)\right]^{-2} r_p \tag{A3}$$

The corrected crack length and the gage-indicated crack length are related from equations (A1) and (A3) by

$$\frac{a}{a_g} = \frac{1}{1 + \left[1 + \left(\frac{2}{\pi}\right)^4 \left(\frac{\epsilon_{fg}}{\epsilon_{yY}} - 1\right)\right]^{-2} \frac{r_p}{a}} \tag{A4}$$

For a plate of width W, r_p/a is given in equation 2-28 of reference 13 as a function of the ratio of gross normal stress σ to the stress at the elastic-plastic interface σ_{yY} by

$$\frac{r_p}{a} = \frac{W}{\pi a} \arcsin\left(\sin\frac{\pi a}{W} \sec\frac{\pi\sigma}{2\sigma_{yY}}\right) - 1 \tag{A5}$$

For an infinitely wide plate, equation (A5) reduces to

$$\frac{r_p}{a} = \sec\frac{\pi\sigma}{2\sigma_{yY}} - 1 \tag{A6}$$

The ratio a/a_g can be calculated as a function of σ/σ_{yY} (or σ/σ_{YB} when σ_{yY} is taken as the biaxial yield strength) from equations (A3), (A4), and (A6)

$$\frac{a}{a_g} = \left\{1 + \left[1 + \left(\frac{2}{\pi}\right)^4 \left(\frac{\epsilon_{fg}}{\epsilon_{yY}} - 1\right)\right]^{-2} \left[\frac{W}{\pi a} \arcsin\left(\sin\frac{\pi a}{W} \sec\frac{\pi\sigma}{2\sigma_{yY}}\right) - 1\right]\right\}^{-1} \tag{A7}$$

For $a/W \ll 1$,

$$\frac{a}{a_g} = \left\{1 + \left[1 + \left(\frac{2}{\pi}\right)^4 \left(\frac{\epsilon_{fg}}{\epsilon_{yY}} - 1\right)\right]^{-2} \left(\sec\frac{\pi\sigma}{2\sigma_{yY}} - 1\right)\right\}^{-1} \tag{A8}$$

The continuity gage failure strain ϵ_{fg} was measured from a tensile test of the gage mounted on an aluminum tensile specimen. The measured strain at which the continuity gage failed was taken as ϵ_{fg}. In equations (A7) and (A8), the stress at the elastic-plastic interface σ_{yY} was taken as the 2:1 biaxial yield strength σ_{YB} for the reasons discussed on page 52 of reference 13. The strain at the elastic-plastic interface ϵ_{yY} is computed as $\frac{1 - \nu^2}{E} \sigma_{yY}$ in the same reference.

This theoretical ratio is plotted in figure 12 and is compared to experimental measurements of a/a_g for ELI 5Al-2.5Sn-Ti and 2014-T6 Al flat sheet specimens at -320° F. The agreement is good enough to permit the use of equations (A7) or (A8) to correct the continuity gage readings.

APPENDIX B

CALCULATION OF AVERAGE BULGE COEFFICIENT

A least-square method is selected to compute an average value of C from the set of experimental values C_i. Since the observed C_i do not all have the same precision, the squares of the deviations are weighted by factors w_i (ref. 14). The sum of the weighted squares is

$$s = \sum_{i=1}^{n} w_i (C_i - C)^2 \tag{B1}$$

When minimized, equation (B1) is

$$\frac{\partial s}{\partial C} = 0 = -2 \sum_{i=1}^{n} w_i (C_i - C) \tag{B2}$$

and at the minimum

$$C = \frac{\sum_{i=1}^{n} w_i C_i}{\sum_{i=1}^{n} w_i} \tag{B3}$$

If the C_i values are weighted such that the values of w_i are inversely proportional to the square of the expected error ΔC caused by error in crack length and toughness (eq. (C9) in appendix C),

$$w_i \alpha \left(\frac{1}{|\Delta C|_i} \right)^2 \tag{B4}$$

and

$$C = \frac{\sum_{i=1}^{n} \frac{C_i}{\left(|\Delta C|_i\right)^2}}{\sum_{i=1}^{n} \frac{1}{\left(|\Delta C|_i\right)^2}} \tag{B5}$$

where $|\Delta C|$ is given by equation (C9).

APPENDIX C

ERROR IN BULGE COEFFICIENT

Because values of the bulge coefficient computed from equations (18) and (19) are highly dependent upon the crack length and the fracture toughness, an error in C is presumed to be due mainly to error in these two parameters. The magnitude of the largest difference in C expected from changes in K_c and a is

$$|\Delta C| = \left|\frac{\partial C}{\partial a}\Delta a\right| + \left|\frac{\partial C}{\partial K_c}\Delta K_c\right| \tag{C1}$$

From equation (18),

$$\frac{\partial C}{\partial a_c} = -\frac{C}{a_c}\left(\frac{1+\dfrac{R}{Ca_c}}{2+\dfrac{1}{\pi a_c}\dfrac{K_c^2}{\sigma_{YB}^2}}\right) \tag{C2}$$

and

$$\frac{\partial C}{\partial K_c} = \frac{2C}{K_c}\left(\frac{1+\dfrac{R}{Ca_c}}{2+\dfrac{1}{\pi a_c}\dfrac{K_c^2}{\sigma_{YB}^2}}\right) \tag{C3}$$

Consequently,

$$|\Delta C| = \frac{C}{a_c}\left(\frac{1+\dfrac{R}{Ca_c}}{2+\dfrac{1}{\pi a_c}\dfrac{K_c^2}{\sigma_{YB}^2}}\right)|\Delta a_c| + \frac{2C}{K_c}\left(\frac{1+\dfrac{R}{Ca_c}}{2+\dfrac{1}{\pi a_c}\dfrac{K_c^2}{\sigma_{YB}^2}}\right)|\Delta K_c| \tag{C4}$$

An error in measurement of K_c due to an error Δa_c is given by $(\partial K_c/\partial a_c)\Delta a_c$. In a flat-sheet toughness test K_c is related to a_c by

$$K_c = \sigma_c \sqrt{\pi a_c + \frac{1}{2} \frac{K_c^2}{\sigma_Y^2}} \tag{C5}$$

if the width effect is ignored. Then,

$$\frac{\partial K_c}{\partial a} = \frac{K_c}{2a_c} \tag{C6}$$

When $\mathcal{E}$, the fractional error in K_c due to material inconsistencies is included, the total error ΔK_c is

$$\Delta K_c = \frac{K_c}{2a_c} \Delta a_c + \mathcal{E} K_c \tag{C7}$$

and

$$\frac{\Delta K_c}{K_c} = \left(\frac{\Delta a_c}{2a_c}\right)_T + \mathcal{E} \tag{C8}$$

where the subscript T refers to a flat-sheet toughness test.

The fractional error in C as given by equation (C4) is then

$$\frac{|\Delta C|}{C} = \left|\frac{\Delta a_c}{a_c}\right| + \left(\left|\frac{\Delta a_c}{a_c}\right| + \left|\frac{\Delta a_c}{a_c}\right|_T + 2|\mathcal{E}|\right)\left(\frac{1 + \frac{R}{Ca_c}}{2 + \frac{1}{\pi a_c} \frac{K_c^2}{\sigma_{YB}^2}}\right) \tag{C9}$$

or, when the correlation is based on initial crack length and nominal fracture toughness, the fractional error in C is

$$\frac{\Delta C}{C} = \left|\frac{\Delta a_o}{a_o}\right| + \left(\left|\frac{\Delta a_o}{a_o}\right| + \left|\frac{\Delta a_o}{a_o}\right|_T + 2|\mathcal{E}|\right)\left(\frac{1 + \frac{R}{Ca_c}}{2 + \frac{1}{\pi a_o}\frac{K_{cn}^2}{\sigma_{YB}^2}}\right) \qquad \text{(C10)}$$

The error in C was computed using an estimated Δa of 0.02 inch and a toughness test crack length of 1.0 inch. The estimated fractional error in toughness $|\mathcal{E}|$ was taken as 0.04 for the aluminum and 0.06 for the titanium.

REFERENCES

1. Irwin, G. R.: Fracture. Encyclopedia of Physics. Vol. VI. S. Flugge, ed., Springer-Verlag (Berlin), 1958, pp. 551-590.
2. ASTM Special Committee on Fracture Toughness Testing of High-Strength Metallic Materials: Fracture Testing of High-Strength Sheet Materials. Bull. No. 243, ASTM, Jan. 1960, pp. 29-40.
3. ASTM Special Committee on Fracture Testing of High Strength Metallic Materials: Progress in Measuring Fracture Toughness and Using Fracture Mechanics. Mater. Res. and Stand., vol. 4, no. 3, Mar. 1964, pp. 107-119.
4. Srawley, John E.; and Brown, William F., Jr.: Fracture Toughness Testing. NASA TN D-2599, 1965.
5. Tiffany, C. F.; and Masters, J. N.: Applied Fracture Mechanics. Fracture Toughness Testing and Its Applications. STP No. 381, ASTM, 1964, pp. 249-277.
6. Peters, Roger W.; and Kuhn, Paul: Bursting Strength of Unstiffened Pressure Cylinders with Slits. NACA TN 3993, 1957.
7. Irwin, G. R.: Analysis of Stresses and Strains Near the End of a Crack Traversing a Plate. J. Appl. Mech., vol. 24, no. 3, Sept. 1957, pp. 361-364.
8. Williams, M. L.: On the Stress Distribution at the Base of a Stationary Crack. J. Appl. Mech., vol. 24, no. 1, Mar. 1957, pp. 109-114.
9. Irwin, G. R.: Plastic Zone Near a Crack and Fracture Toughness. Proc. Seventh Sagamore Ord. Materials Conf., Syracuse Univ. Res. Inst., Aug. 1960.
10. Getz, David F.; Pierce, William S.; Calvert, Howard F.: Correlation of Uniaxial Notch Tensile Data with Pressure-Vessel Fracture Characteristics. Paper No. 63-WA-187, ASME, 1963.
11. Kemp, R. H.: Characteristics and Application of Foil Strain Gages at -423° F. Paper Presented at Western Regional Strain Gage Conference, Denver (Colo.), Sept. 30-Oct. 1, 1963.
12. Lacey, G. C.: The Residual Static Strength of Structures Containing Cracks. Rept. No. ARL/SM-288, Aeron. Res. Labs., Melbourne (Australia), Apr. 1962.
13. Anderson, R. B.: Plastic Flow at the Tip of a Crack Related to Fracture Mechanics. Ph. D. Thesis, Carnegie Inst. Tech., June 1964.
14. Wilson, E. Bright, Jr.: An Introduction to Scientific Research. McGraw-Hill Book Co., Inc., 1952.

TABLE I. - CYLINDER BURST TEST DATA

Temperature, °F	Critical hoop stress, σ_{hc}, psi	Initial crack length, $2a_o$, in.	Critical crack length indicated by continuity gage, $2a_g$, in.	Corrected critical crack length, $2a_c$, in.
2014-T6 Al				
-423	82 200	0.104	(a)	(a)
	63 400	.250		
	39 600	.500		
	32 000	.750		
	21 000	1.000		
	19 800	1.250		
	13 200	1.750		
	11 900	2.000		
-320	71 600	0.113	(a)	(a)
	70 600	.150	0.450	0.250
	63 700	.200	.430	.282
	58 500	.250	.430	.310
	52 200	.300	.520	.402
	47 400	.400	.620	.512
	40 100	.500	.760	.670
	30 200	.750	1.002	.952
	23 100	1.000	1.280	1.236
	18 600	1.250	1.410	1.380
	14 400	1.750	1.940	1.914
	11 300	2.000	2.120	2.100
Room	64 400	0.114	(a)	(a)
	34 000	.500	0.670	0.586
	20 600	1.000	(a)	(a)
	9 700	2.000	2.160	2.130

Temperature, °F	Critical hoop stress, σ_{hc}, psi	Initial crack length, $2a_o$, in.	Critical crack length indicated by continuity gage, $2a_g$, in.	Corrected critical crack length, $2a_c$, in.
5Al-2.5Sn-Ti				
-423	171 500	0.093	(b)	(b)
	160 900	.155		
	133 300	.190		
	121 400	.277		
	114 200	.280		
	84 600	.523		
	76 000	.482		
	63 600	.803		
	63 000	.941		
	61 500	.762		
	51 600	.985		
	40 600	1.600		
	37 700	1.560		
-320	190 400	0.125	0.300	0.125
	164 900	.241	(a)	(a)
	156 600	.229	.420	.250
	115 500	.440	.780	.616
	105 100	.453	.530	.440
	84 900	.733	.960	.880
	74 600	.765	.860	.790
	71 800	.946	1.160	1.080
	66 200	.991	1.260	1.180
	44 100	1.480	1.770	1.720
	35 900	1.460	1.660	1.620

[a] Slow crack growth was not measured.

[b] No detectable slow crack growth occurred.

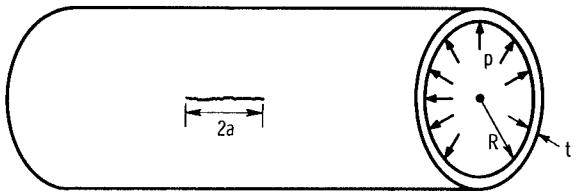

Figure 1. - Cracked pressurized cylinder.

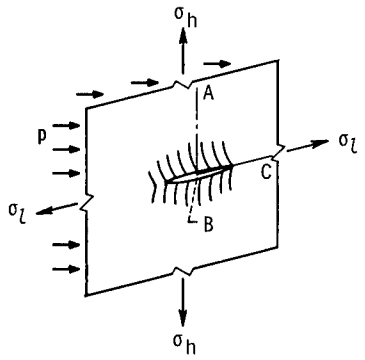

(a) Bulging near through-crack due to lateral pressure.

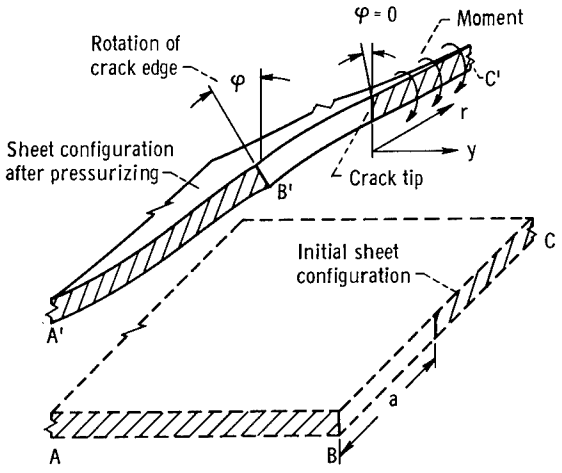

(b) Section ABC showing rotation of crack edge and resulting moment ahead of the crack.

Figure 2. - Distortion of material near through-crack in sheet subjected to lateral pressure.

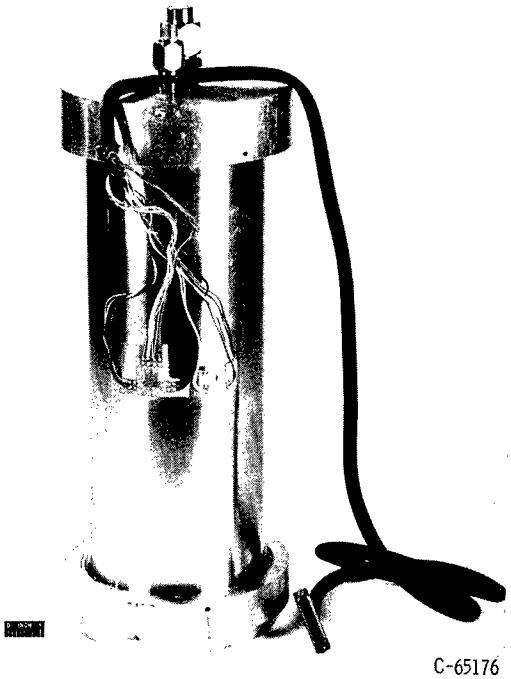

C-65176

Figure 3. - Notched cylindrical burst test specimen.

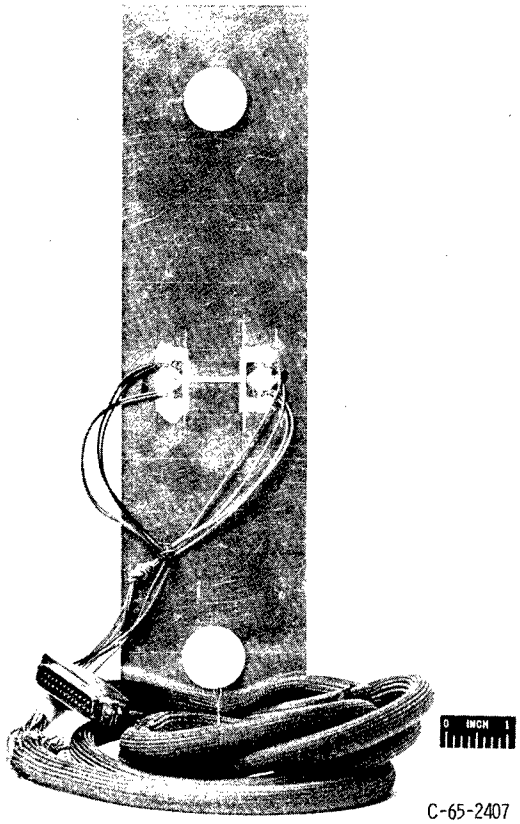

C-65-2407

Figure 4. - Notched flat sheet fracture toughness specimen.

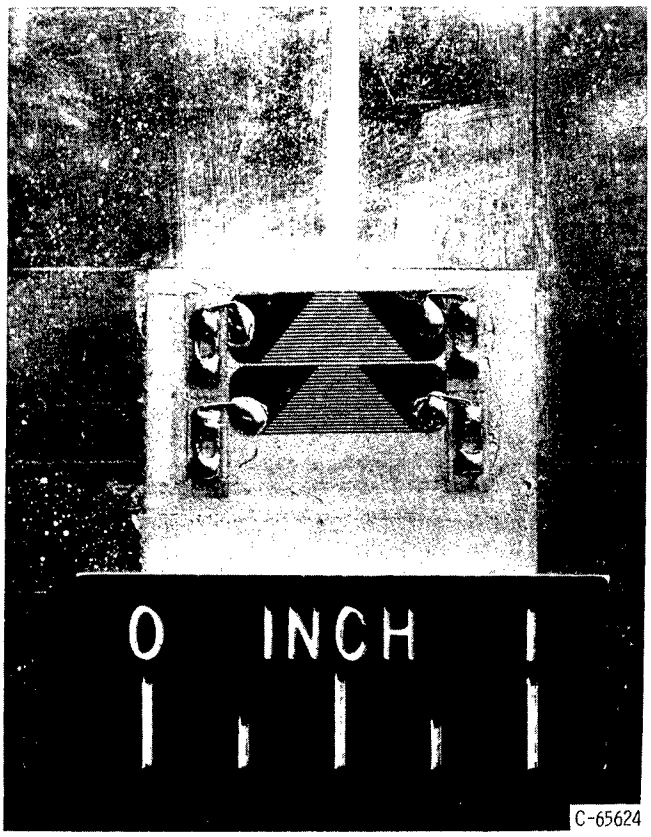

Figure 5. - Foil element continuity gage mounted at notch root.

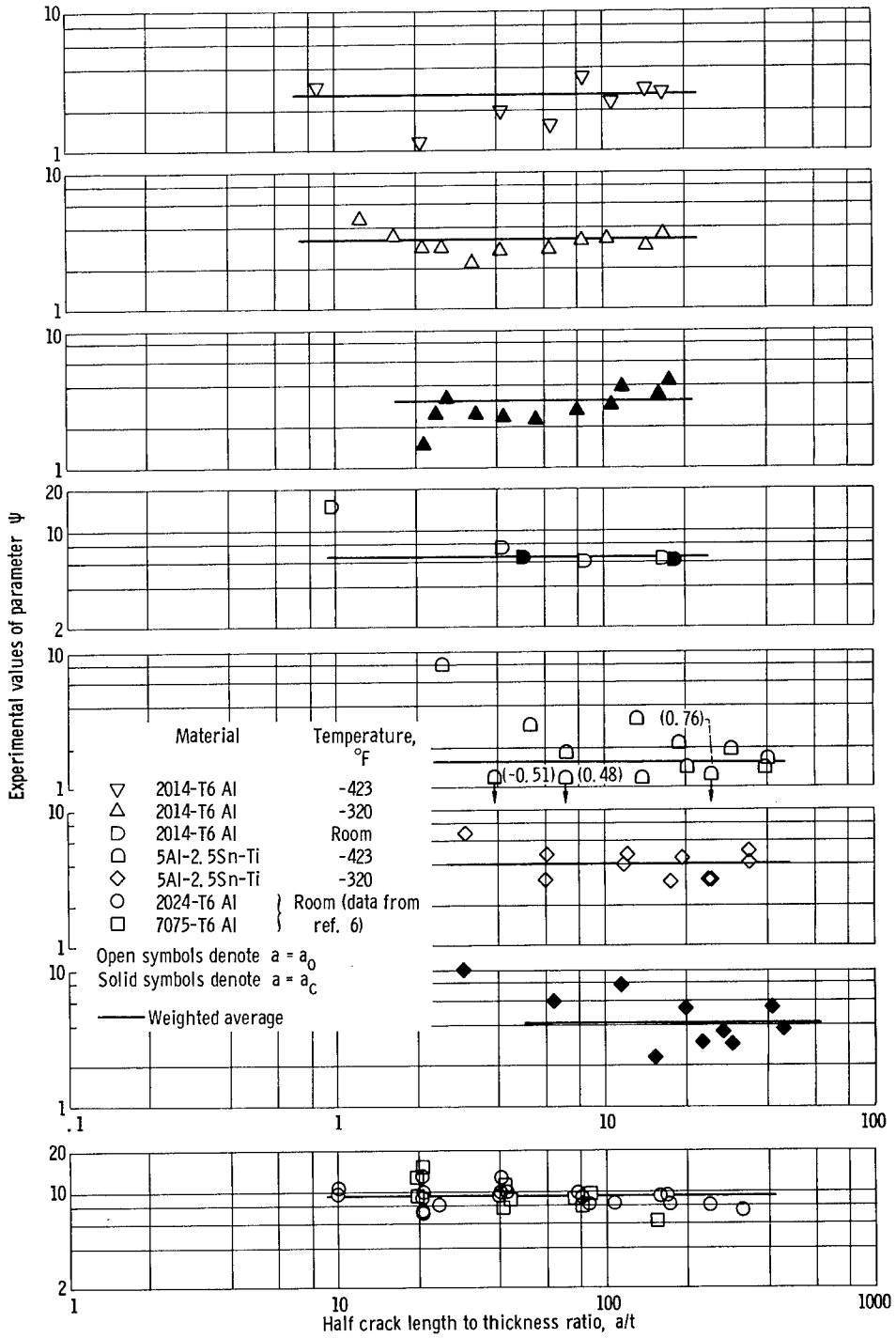

Figure 6. - Influence of half crack length to thickness ratio a/t on parameter ψ.

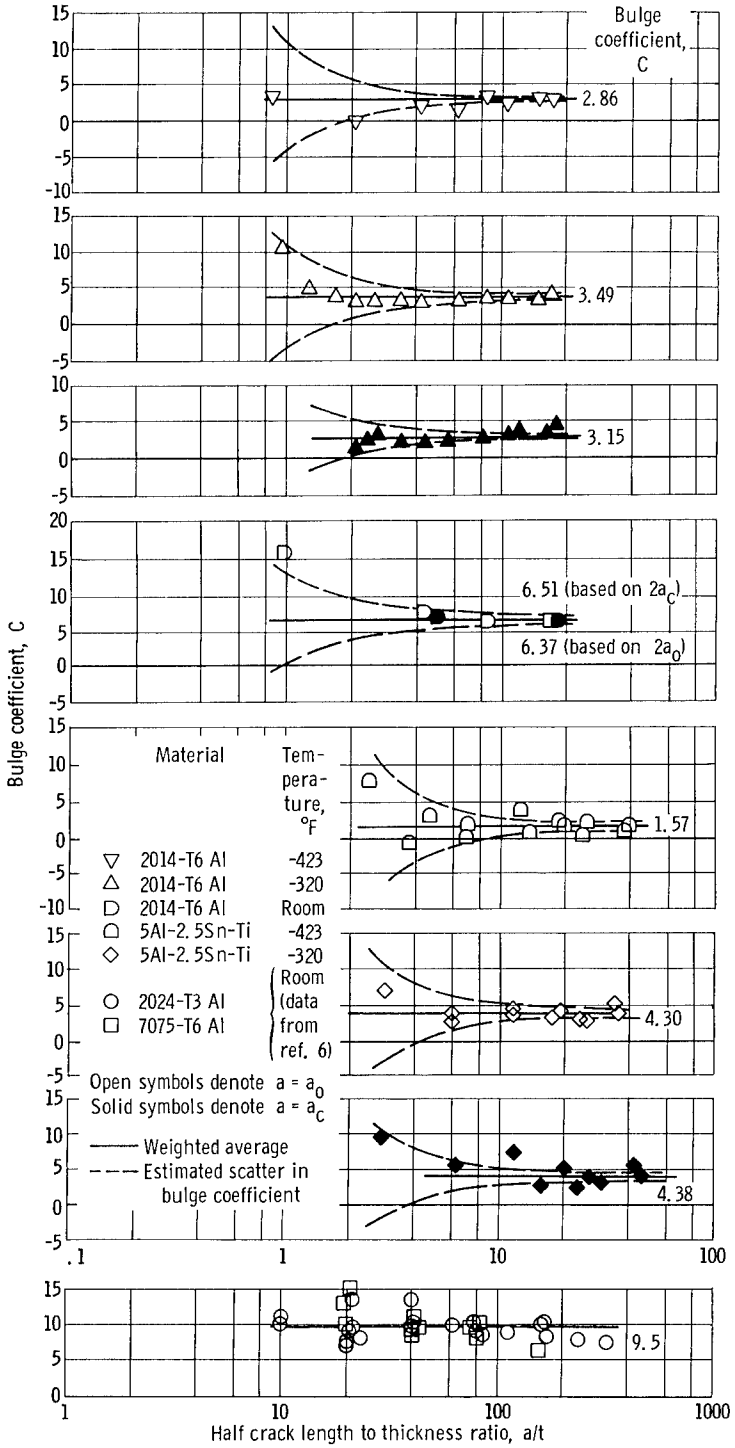

Figure 7. - Bulge coefficient and estimated scatter in computed values.

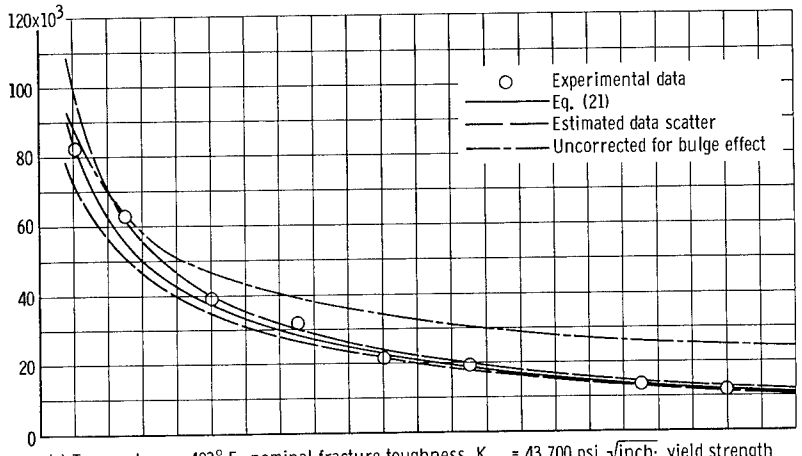

(a) Temperature, -423° F; nominal fracture toughness K_{cn} = 43 700 psi $\sqrt{\text{inch}}$; yield strength σ_{YB} = 104 000 psi; bulge coefficient C = 2.86.

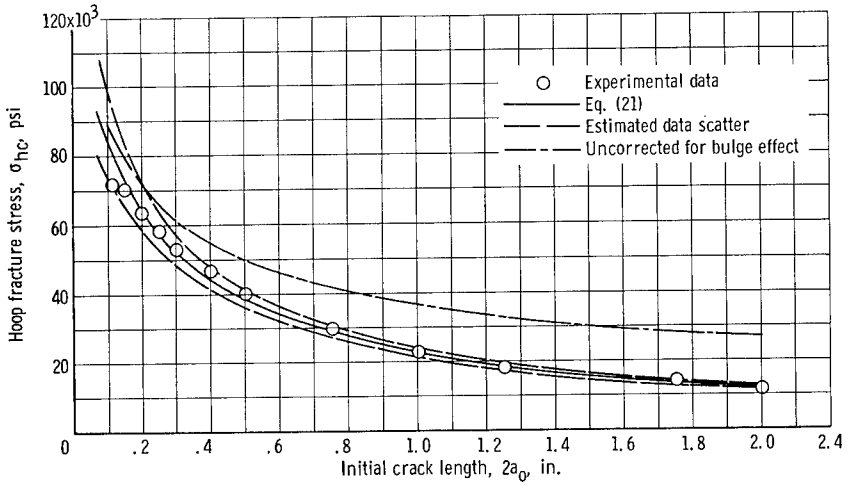

(b) Temperature, -320° F; nominal fracture toughness K_{cn} = 48 500 psi $\sqrt{\text{inch}}$; yield strength σ_{YB} = 94 200 psi; bulge coefficient C = 3.49.

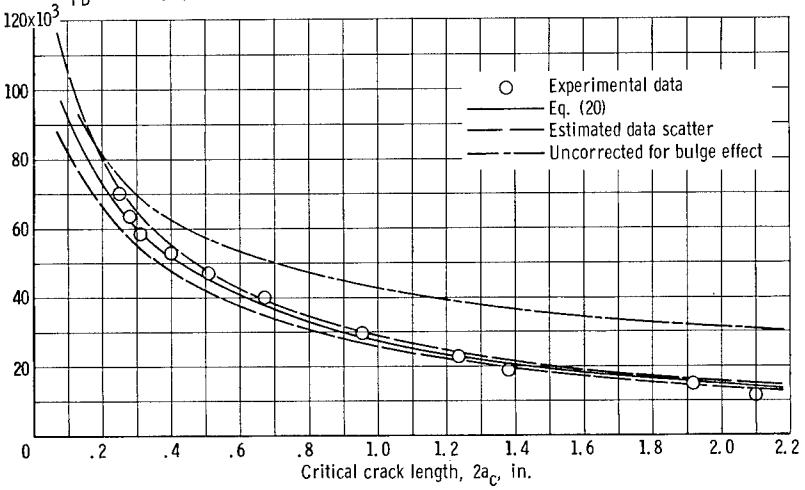

(c) Temperature, -320° F; critical fracture toughness K_c = 56 600 psi $\sqrt{\text{inch}}$; yield strength σ_{YB} = 94 200 psi; bulge coefficient C = 3.15.

Figure 8. - Fracture strength of 2014-T6 Al cylinders. Radius of cylinder R = 2.81 inches.

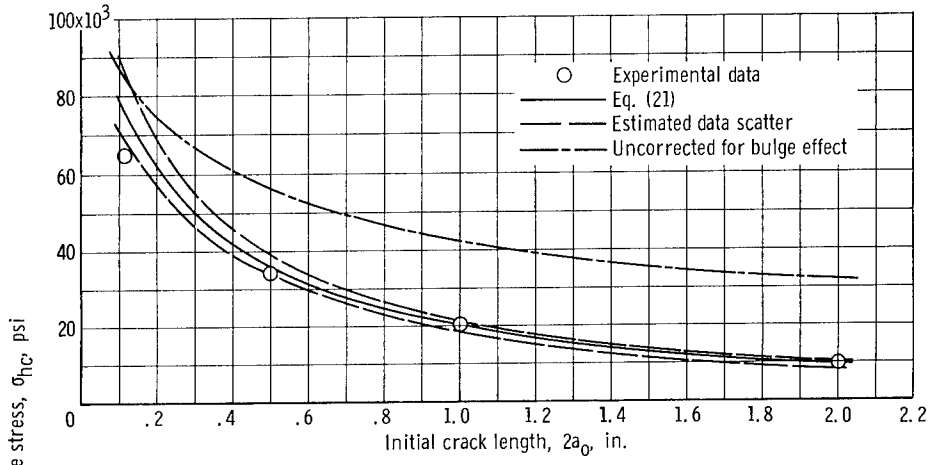

(d) Room temperature; nominal fracture toughness K_{cn} = 58 400 psi $\sqrt{\text{inch}}$; yield strength σ_{YB} = 78 100 psi; bulge coefficient C = 6.37.

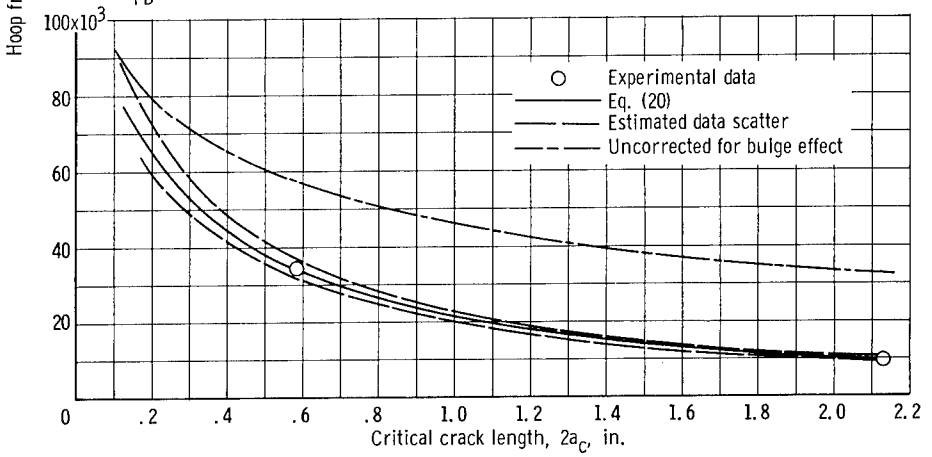

(e) Room temperature; critical fracture toughness K_c = 64 500 psi $\sqrt{\text{inch}}$; yield strength σ_{YB} = 78 100 psi; bulge coefficient C = 6.51.

Figure 8. - Concluded.

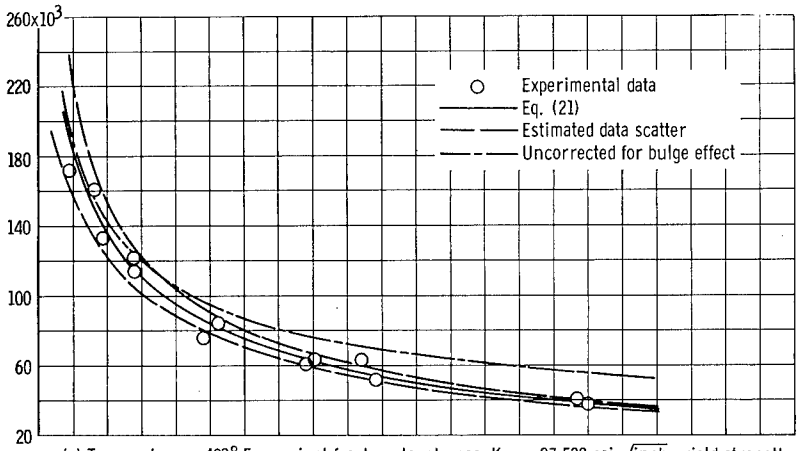

(a) Temperature, -423° F; nominal fracture toughness K_{cn} = 87 500 psi $\sqrt{\text{inch}}$; yield strength σ_{YB} = 252 000 psi; bulge coefficient C = 1.57.

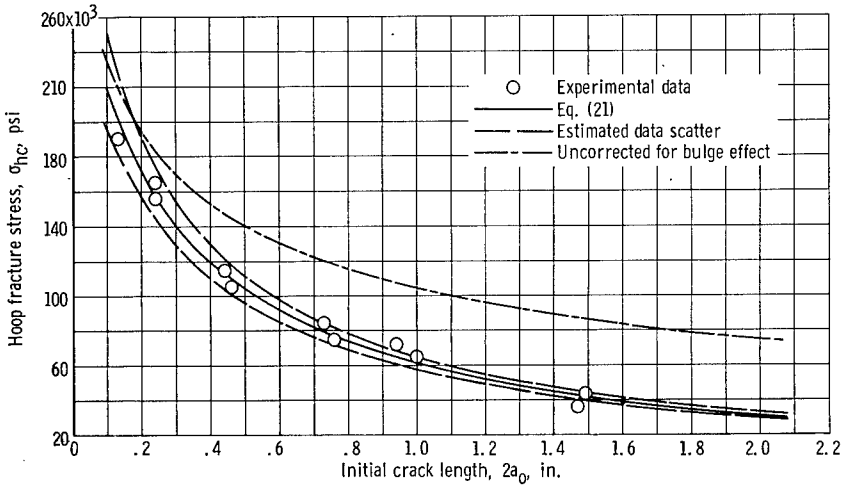

(b) Temperature, -320° F; nominal fracture toughness K_{cn} = 139 000 psi $\sqrt{\text{inch}}$; yield strength σ_{YB} = 222 000 psi; bulge coefficient C = 4.30.

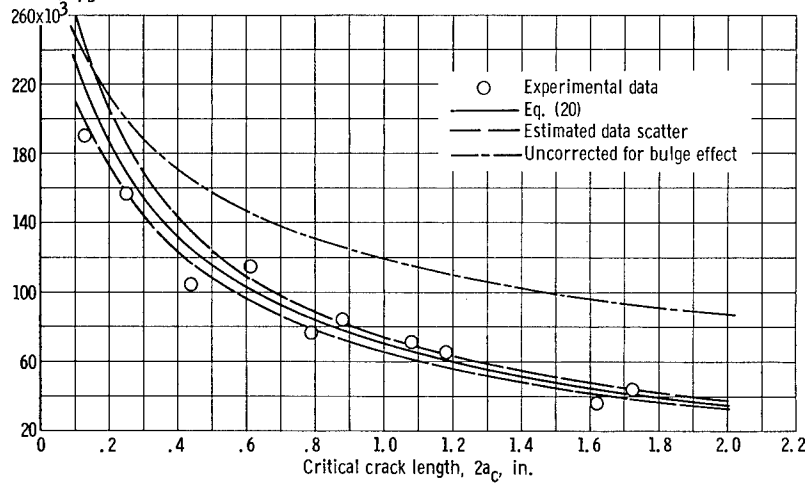

(c) Temperature, -320° F; critical fracture toughness K_c = 160 000 psi $\sqrt{\text{inch}}$; yield strength σ_{YB} = 222 000 psi; bulge coefficient C = 4.38.

Figure 9. - Fracture strength of 5Al-2.5Sn-Ti cylinders. Radius of cylinder R = 3.00 inches.

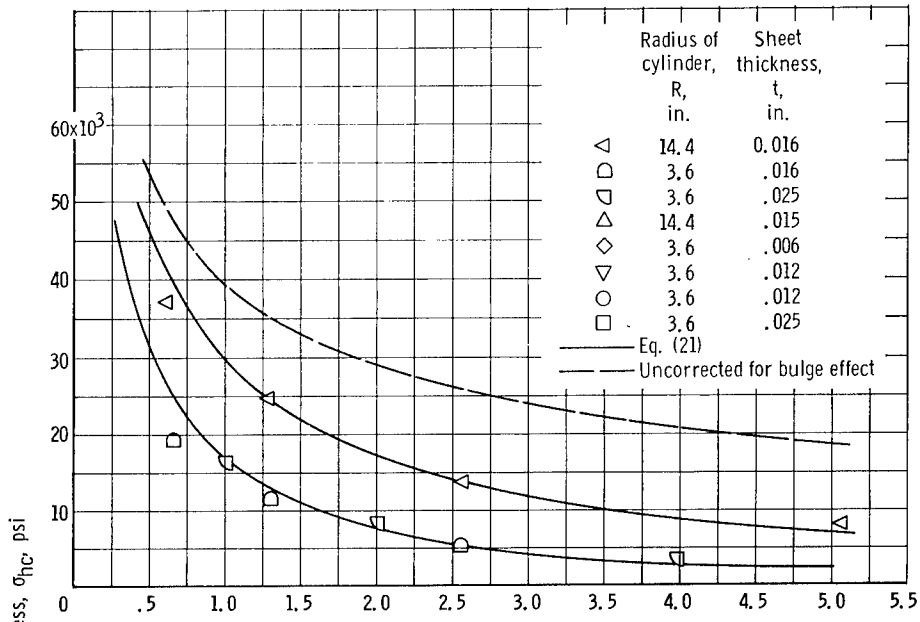

(a) 7075-T6 Al; nominal fracture toughness K_{cn} = 53 000 psi $\sqrt{\text{inch}}$; yield strength σ_{YB} = 75 000 psi.

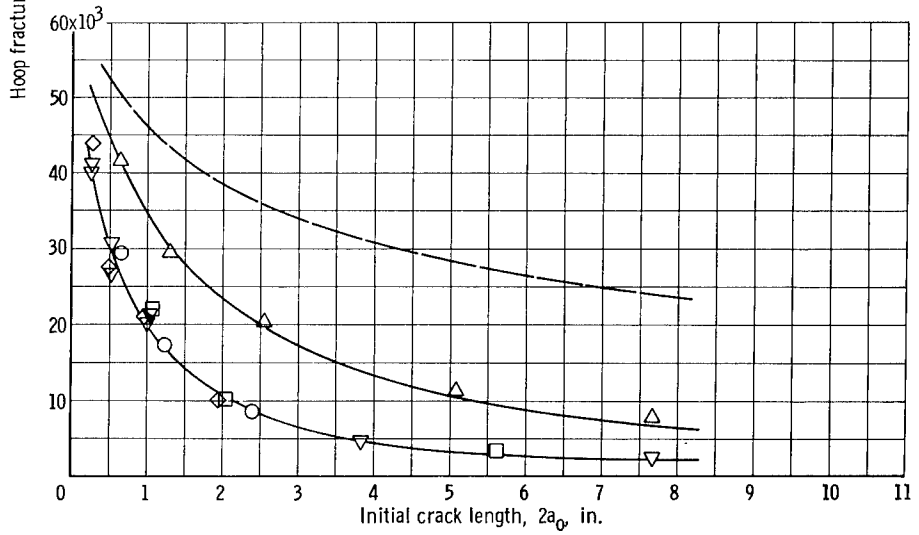

(b) 2024-T3 Al; nominal fracture toughness K_{cn} = 90 000 psi $\sqrt{\text{inch}}$; yield strength σ_{YB} = 42 000 psi.

Figure 10. - Fracture strength of aluminum tanks at room temperature. Bulge coefficient C = 9.5. (Data taken from ref. 6.)

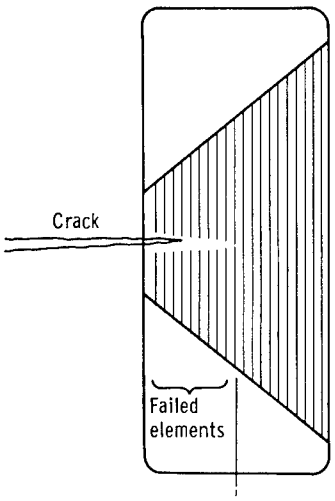

(a) Foil element continuity gage.

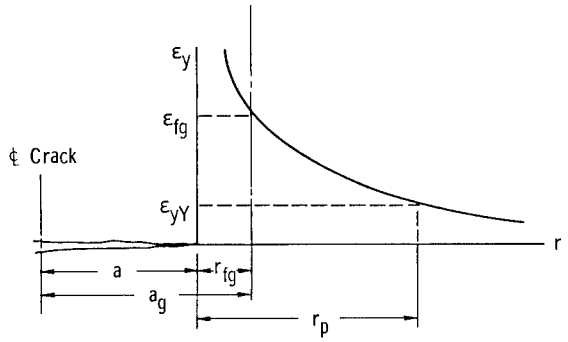

(b) Strain ahead of crack.

Figure 11. - Failure of continuity gage elements ahead of crack front.

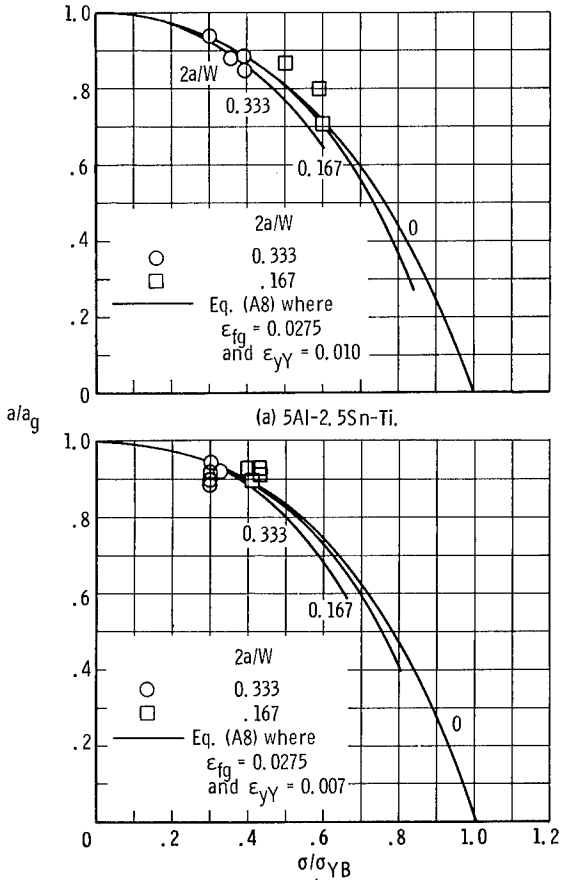

(b) 2014-T6 Al.

Figure 12. - Continuity gage calibration. Temperature, -320° F.